

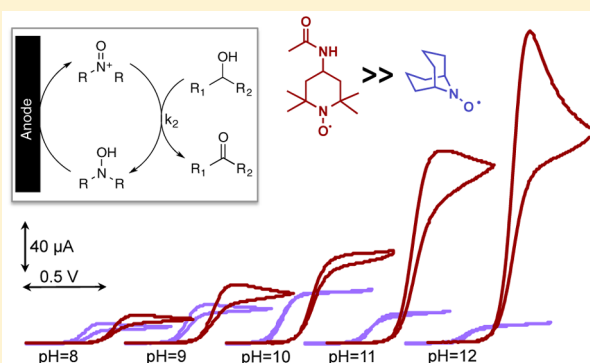
Electrocatalytic Alcohol Oxidation with TEMPO and Bicyclic Nitroxyl Derivatives: Driving Force Trumps Steric Effects

Mohammad Rafiee, Kelsey C. Miles, and Shannon S. Stahl*

Department of Chemistry, University of Wisconsin—Madison, 1101 University Avenue, Madison, Wisconsin 53706, United States

S Supporting Information

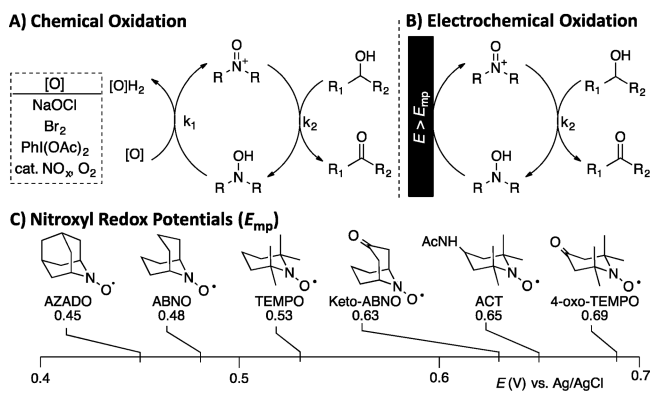
ABSTRACT: Bicyclic nitroxyl derivatives, such as 2-azaadamantane *N*-oxyl (AZADO) and 9-azabicyclo[3.3.1]nonane *N*-oxyl (ABNO), have emerged as highly effective alternatives to TEMPO-based catalysts for selective oxidation reactions (TEMPO = 2,2,6,6-tetramethyl-1-piperidine *N*-oxyl). Their efficacy is widely attributed to their smaller steric profile; however, electrocatalysis studies described herein show that the catalytic activity of nitroxyls is more strongly affected by the nitroxyl/oxoammonium redox potential than by steric effects. The inexpensive, high-potential TEMPO derivative, 4-acetamido-TEMPO (ACT), exhibits higher electrocatalytic activity than AZADO and ABNO for the oxidation of primary and secondary alcohols. Mechanistic studies provide insights into the origin of these unexpected reactivity trends. The superior activity of ACT is especially noteworthy at high pH, where bicyclic nitroxyls are inhibited by formation of an oxoammonium hydroxide adduct.



INTRODUCTION

TEMPO (2,2,6,6-tetramethyl-1-piperidine *N*-oxyl) and related nitroxyl derivatives are important catalysts for alcohol oxidation,¹ and they find widespread use in industrial² and laboratory³ applications (Scheme 1). Diverse stoichiometric

Scheme 1. Chemical and Electrochemical Alcohol Oxidation Methods with Nitroxyls of Different Structures and Redox Potentials

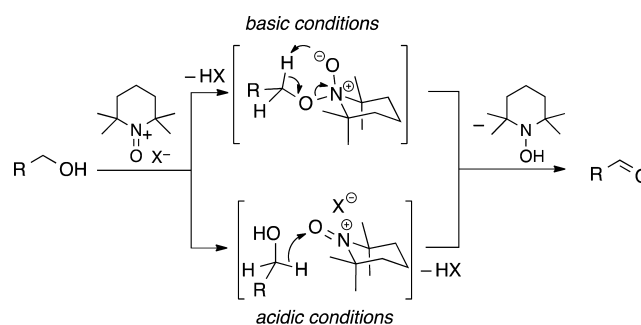


oxidants have been used to promote catalytic turnover, the most common of which include bleach (NaOCl), hypervalent iodine reagents, and O₂ in combination with NO_x co-catalysts (Scheme 1A).^{1–3} In addition to these chemical oxidation methods, nitroxyls have been widely studied as mediators for electrocatalytic alcohol oxidation (Scheme 1B).^{4,5} The latter

approach has important implications for energy conversion applications, as demonstrated in recent studies of photoelectrochemical conversion of biomass⁴ⁱ and biofuel cells.^{4b,i}

Under typical (basic) reaction conditions, TEMPO exhibits strong steric discrimination in its reaction with alcohols, including the ability to achieve chemoselective oxidation of primary (1°) alcohols in the presence of unprotected secondary (2°) alcohols.⁶ This selectivity has been attributed to steric effects in the formation of an alkoxide adduct with the oxoammonium species (Scheme 2, top pathway).^{1b} The selectivity changes when the reaction is performed under acidic conditions, wherein the mechanism is proposed to involve bimolecular hydride transfer, which favors more-electron-rich

Scheme 2. Proposed Mechanisms for TEMPO⁺-Mediated Oxidation of Alcohols under Different Conditions



Received: September 14, 2015

Published: October 27, 2015

substrates (i.e., $2^\circ > 1^\circ$ alcohols).⁷ The reactions under the acidic conditions are typically considerably slower than those under basic conditions, however.

Recently, significant advances in nitroxyl-catalyzed alcohol oxidation have been made through the use of bicyclic nitroxyls, such as 2-azaadamantane *N*-oxyl (AZADO) and 9-azabicyclo-[3.3.1]nonane *N*-oxyl (ABNO) (cf. Scheme 1C).⁸ These nitroxyls exhibit excellent activity for the oxidation of both 1° and 2° alcohols, and their favorable catalytic properties are primarily attributed to the reduced steric hindrance around the active nitroxyl/oxoammonium site. Unfortunately, the cost or multi-step syntheses of these reagents constrain their use, especially for large-scale applications.⁹

Building on our studies of nitroxyl (co-)catalyzed aerobic oxidation reactions,¹⁰ we recently began exploring electrocatalytic reactions with nitroxyl mediators.¹¹ Whereas TEMPO has been studied extensively as an electrocatalyst for alcohol oxidation,^{4,5} much less attention has been given to the bicyclic nitroxyls.^{4g,8c} The mid-point potential (E_{mp}) of the one-electron nitroxyl/oxoammonium couple varies, depending on the nitroxyl structure (i.e., mono- vs bicyclic) and/or substituents (Scheme 1C),¹² but the effect of the nitroxyl redox potentials on catalytic activity and their implications for chemical and electrochemical oxidation methods have not been addressed. Here, we describe the electrocatalytic behavior of a series of bicyclic and TEMPO-based nitroxyls. Free-energy correlations show that nitroxyl-catalyzed alcohol oxidation rates under chemical vs electrochemical conditions exhibit opposite trends with respect to the nitroxyl/oxoammonium redox potential. Mechanistic studies reveal the origin of this unexpected inversion of activity, and the results have important implications for practical applications of nitroxyl-based alcohol oxidation reactions. For example, the low-cost, readily accessible 4-acetamido-TEMPO (ACT) outperforms the more-expensive bicyclic nitroxyls under electrochemical conditions.

RESULTS AND DISCUSSION

Kinetic Analysis of Electrocatalytic Oxidation of Alcohols with Different Nitroxyls. Cyclic voltammograms (CVs) of AZADO (a), ABNO (b), TEMPO (c), and ACT (d) reveal reversible electron transfer under conditions similar to those commonly used for alcohol oxidation (Figure 1A). In contrast, keto-ABNO and 4-oxo-TEMPO exhibit irreversible behavior under these basic conditions (cf. trace e in Figure 1A), reflecting the instability of the corresponding oxoammonium species. Keto-substituted oxoammonium species have been

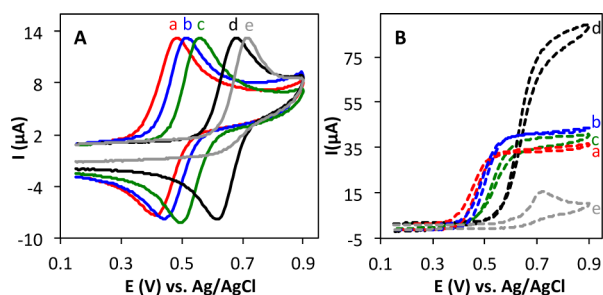


Figure 1. Cyclic voltammograms of 1 mM AZADO (a), ABNO (b), TEMPO (c), ACT (d), and 4-oxo-TEMPO (e) in the absence (A) and presence (B) of 50 mM 1-butanol in $\text{HCO}_3^-/\text{CO}_3^{2-}$ electrolyte (pH 10), scan rate 50 mV s^{-1} .

shown to be highly susceptible to base-promoted ring opening.¹³ ACT exhibits the highest mid-point potential ($E_{mp} = 0.65 \text{ V}$) among the four electrochemically reversible nitroxyls.

CVs of the nitroxyls were then reacquired with 50 mM 1-butanol present in the solutions (Figure 1B). The S-shaped CVs, showing a significant increase in the oxidation peak and a disappearance of the reduction peak, are diagnostic of electrocatalysis, and the oxidation current is proportional to the catalytic turnovers that occur on the CV time scale. AZADO, ABNO, and TEMPO perform similarly, while ACT exhibits more than 2-fold higher catalytic current than the other nitroxyls. No significant catalytic activity was observed for 4-oxo-TEMPO, reflecting the instability of the oxoammonium species.

To gain a more-quantitative comparison of the different nitroxyls, the electrocatalytic reactions were evaluated by additional electrochemical studies. Representative chronoamperograms (CAs) obtained with ABNO are shown in Figure 2A. In the absence of alcohol, the CA exhibits an exponential

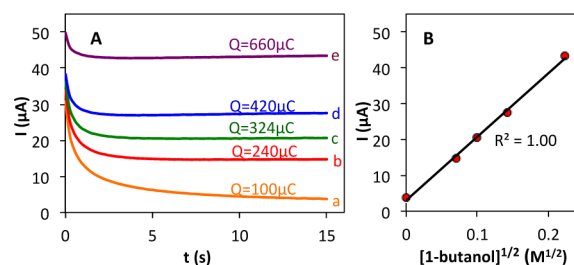
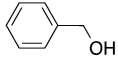
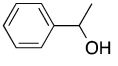
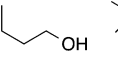
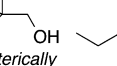
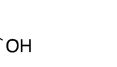


Figure 2. (A) Chronoamperograms of ABNO (1 mM) in the absence (a) and presence of 1-butanol at 5 mM (b), 10 mM (c), 20 mM (d) and 50 mM (e) concentrations in $\text{HCO}_3^-/\text{CO}_3^{2-}$ electrolyte (pH 10). (B) Plot of current vs $[\text{1-butanol}]^{1/2}$ with an applied potential 0.7 V vs Ag/AgCl.

decay (curve a), consistent with diffusion-controlled oxidation of the nitroxyl to the oxoammonium. The CA current increases upon addition of 1-butanol, and the steady-state current is proportional to the square root of the alcohol concentration (Figure 2A, curves b–e).¹⁴ Similar studies were performed for each of the other nitroxyls (AZADO, TEMPO, and ACT) in order to compare their catalytic activities and turnover frequencies (TOFs) (see Figures S1–S4).

The difference between the current in the presence and absence of 1-butanol (i.e., curves b–e vs curve a in Figure 2A) is directly proportional to the nitroxyl TOF. The TOFs for each of the four nitroxyls with a series of five different alcohols are presented in Table 1. The alcohol substrates were selected as

Table 1. TOF (h^{-1}) of Different Nitroxides for Oxidation of Alcohols^a

					
	1° benzylic	2° benzylic	1° aliphatic	sterically hindered 1° aliphatic	2° aliphatic
ABNO	1088	238	588	337	87
AZADO	1128	358	488	298	78
TEMPO	853	118	568	198	18
ACT	1228	378	708	388	73

^aStandard conditions for TOF determination: 50 mM alcohol, 1.0 mM nitroxyl, $\text{HCO}_3^-/\text{CO}_3^{2-}$ electrolyte (pH 10).

representative examples of 1° and 2° benzylic, 1° and 2° aliphatic, and sterically hindered 1° aliphatic alcohols. The data show that ACT is nearly always the most active catalyst. The only exception was evident in the oxidation of 2-butanol, but even in this case, the activity of ACT is comparable to those of ABNO and AZADO. TEMPO exhibits the lowest activity in all cases, except for the oxidation of 1-butanol, for which AZADO is the least active. Most significantly, the activity of ACT is much higher than expected from recent literature reports that highlight the predominant role of steric effects.⁸

Analysis of pH Effects on Electrocatalytic Oxidation of Alcohols with Different Nitroxyls. The advantageous performance of ACT relative to the bicyclic nitroxyls is even more evident when ACT and ABNO are compared at different pH values (Figure 3A). CVs were obtained for the oxidation of

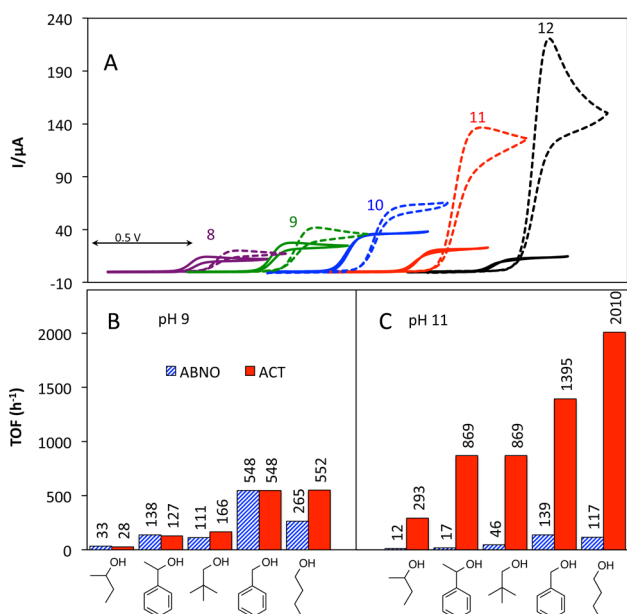


Figure 3. (A) Cyclic voltammograms of ABNO (solid line) and ACT (dashed line) in the presence of 50 mM 1-butanol at various pH values, scan rate 50 mV s⁻¹. (B,C) TOFs (h⁻¹) of ACT and ABNO for oxidation of various alcohols: 1 mM ACT or ABNO, 50 mM alcohol in aqueous carbonate buffers; (B) 0.14 M NaHCO₃ and 0.01 M Na₂CO₃ for pH 9; (C) 0.02 M NaHCO₃ and 0.13 M Na₂CO₃ for pH 11.

1-butanol by ACT reveal a significant increase in the catalytic current upon raising the pH from 8 to 12 (dashed CVs, Figure 3A). ABNO activity is lower than the ACT activity (solid CVs, Figure 3A), and while it increases upon raising the pH from 8 to 10, it then decreases at pH 11 and 12. A comparison of the ACT and ABNO TOFs for five different alcohols at pH 9 and 11 is shown in Figure 3B,C. These data demonstrate the strong impact of pH on catalyst activity, and show that increasing the pH significantly activates ACT, while it strongly suppresses ABNO activity. The pH trend for ACT continues beyond pH 12, and TOFs reach values above 1000 and 6000 h⁻¹ for 2-butanol and 1-butanol, respectively, at pH 13. The effectiveness of ACT as an electrocatalyst was confirmed in bulk electrolysis experiments. Electrochemical oxidation of each of the five alcohols were performed on 1 mmol scale at pH 10 with 2 mol % ACT, and the oxidized products were obtained in 88–98% yields within 2 h at room temperature (Table 2).¹⁵ ABNO exhibits lower activity and is less stable under the same reaction conditions. For example, use of 2 mol% ABNO only achieves

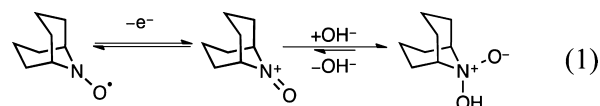
Table 2. Bulk Electrolysis Data for ACT-Mediated Oxidation of Alcohols^a

Reactant:					
Product:					
Time	2 h	2 h	2 h	2 h	2 h
Yields ^b	88%	88%	98%	98%	95%

^aConditions: 0.1 M alcohol in 10 mL of aqueous carbonate buffer, 0.075 M NaHCO₃, 0.075 M Na₂CO₃ (pH 10), 2 mol% ACT, electrolysis at 0.75 V vs Ag/AgCl. ^bNMR yields (internal standard = mesitylene).

47% conversion to benzaldehyde prior to complete loss of catalytic activity.

Several lines of evidence suggest that the decrease in electrocatalytic activity of ABNO above pH 10 arises from its susceptibility to formation of an oxoammonium hydroxide adduct, ABNOOH (eq 1). Adducts of this type have been



described previously for TEMPO⁺ at pH >12.¹⁶ Ring-strain considerations probably account for the increased susceptibility of bicyclic oxoammonium species to such adduct formation. Insights into this adduct formation were obtained from CVs of ABNO at pH 9, 10, and 11, which show that the E_{mp} shifts negative and the reduction peak decreases upon increasing the pH (Figure 4A). These data and CVs at different scan rates

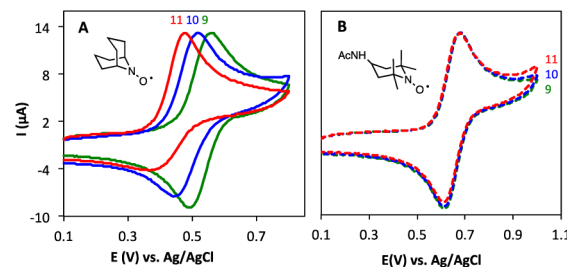


Figure 4. Cyclic voltammograms of ABNO (A) and ACT (B) from pH 9 to 11 (scan rate 50 mV s⁻¹).

(Figure S5) indicate that ABNO⁺ undergoes a chemical reaction upon its electrochemical generation at pH >9. In contrast, CVs of ACT are unaffected by changes to the solution pH (Figure 4B), indicating that ACT and ACT⁺ are stable under the voltammetry conditions. Steric effects, as well as reduced ring strain, probably contribute to the enhanced stability of ACT⁺ at high pH.

Spectroelectrochemical Analysis of ABNO Oxidation at Different pH Values. UV–visible spectroelectrochemical studies complement the voltammetric data and support the hypothesis in eq 1. Well-behaved isosbestic behavior is observed for the redox interconversion of ABNO/ABNO⁺ at pH 8 (Figure 5). Near-isosbestic behavior is also observed at pH 10.2, but the product, which is different from ABNO⁺, corresponds to ABNOOH. Subsequent reduction of this

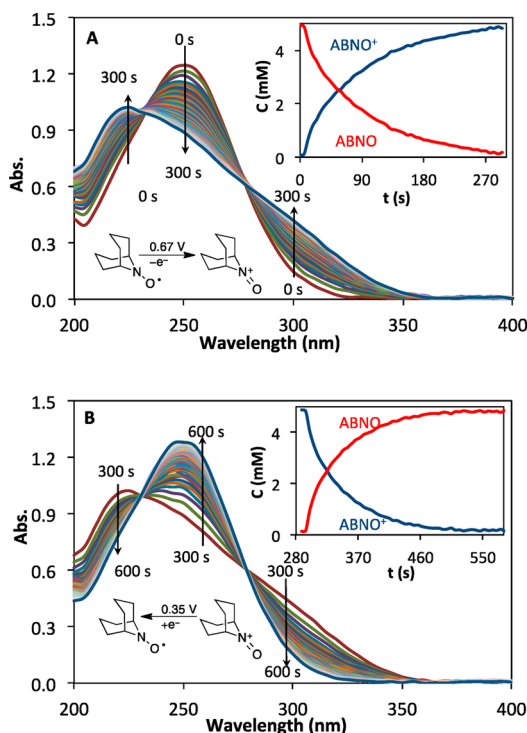


Figure 5. Spectroelectrochemical UV-vis data collected during oxidation of ABNO (A) for 300 s ($t = 0-300$ s), immediately followed by reduction of the in situ generated ABNO⁺ (B) for 300 s ($t = 300-600$ s). Insets: Concentration profiles of ABNO and ABNO⁺ during electrochemical oxidation (A) and reduction (B). Reaction conditions: 0.1 M HCO₃⁻ electrolyte (pH 8.3); oxidation performed at 0.67 V vs Ag/AgCl and reduction at 0.35 V vs Ag/AgCl; spectra recorded every 6 s.

species regenerates ABNO, consistent with reversible formation of the adduct (Figure 6). An equilibrium constant of 3.7×10^4 M⁻¹ was derived for the formation of the ABNOOH from ABNO⁺ and OH⁻ on the basis of the spectroelectrochemical data. At pH >11, oxidation of ABNO is less reversible, possibly reflecting decomposition of ABNOOH under these conditions (Figure S6).

The above data provide a clear rationale for the enhanced activity of ACT relative to bicyclic nitroxyls above pH 10, but we also sought to understand the excellent performance of ACT below pH 10, where bicyclic oxoammonium hydroxide adducts such as ABNOOH do not interfere. Our initial hypothesis was that the high activity of ACT⁺ arises from its high reduction potential (cf. Scheme 1C and Figure 1). Comparisons of TEMPO and bicyclic nitroxyl derivatives are typically performed with chemical oxidants, such as bleach (NaOCl).⁸ In these cases, high-potential nitroxyls (e.g., ACT) could undergo sluggish oxidation by the chemical oxidant, thereby masking their intrinsic alcohol-oxidation reactivity.¹⁷ Low-potential nitroxyls, such as AZADO and ABNO, will therefore experience a competitive advantage.

In Situ Monitoring of Nitroxyl-Catalyzed Oxidation of 1-Butanol by Bleach. AZADO-, ABNO-, TEMPO-, and ACT-catalyzed oxidation of 1-butanol were analyzed with bleach as the oxidant. It was possible to monitor the distribution of catalyst oxidation states during the reaction via cyclic chronoamperometry as an analytical technique. In these experiments, the potential at a rotating disk electrode (RDE) was cycled between 180 mV above and 180 mV below the

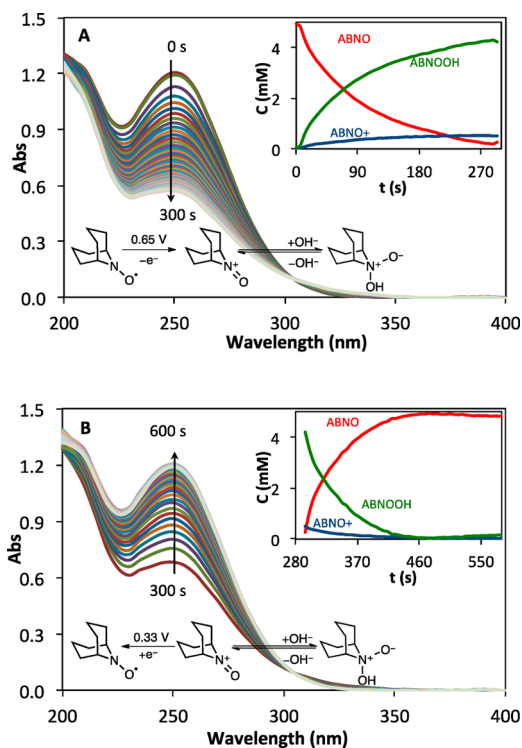


Figure 6. Spectroelectrochemical UV-vis data collected during oxidation of ABNO (A) for 300 s ($t = 0-300$ s), immediately followed by reduction of the in situ generated ABNO⁺/ABNOOH (B) for 300 s ($t = 300-600$ s). Insets: Concentration profiles of ABNO, ABNO⁺, and ABNOOH during electrochemical oxidation (A) and reduction (B). Reaction conditions: HCO₃⁻/CO₃²⁻ electrolyte (pH 10.2); oxidation performed at 0.65 V vs Ag/AgCl and reduction at 0.33 V vs Ag/AgCl; spectra recorded every 6 s.

midpoint potential (E_{mp}) of the nitroxyl. The current measured at $E_{mp} + 180$ mV is proportional to the [nitroxyl], while the current at $E_{mp} - 180$ mV is proportional to the [oxoammonium] (see Figures 7 and S7).

Before analyzing alcohol oxidation reactions, we probed the oxidation of the different nitroxyls by bleach via the cyclic chronoamperometric method described above. Representative data obtained during oxidation of TEMPO by bleach (in the absence of alcohol) is depicted in Figure 7. The data show progressive conversion of TEMPO to TEMPO⁺ over 600 s. The traces with positive current correspond to oxidation of TEMPO at 0.71 V vs Ag/AgCl ($E_{mp} + 180$ mV), and the traces with negative current correspond to reduction of TEMPO⁺ at 0.25 V vs Ag/AgCl ($E_{mp} - 180$ mV) [$E_{mp}(\text{TEMPO}) = 0.53$ V]. Similar data were acquired for the four different nitroxyls, AZADO, ABNO, TEMPO, and ACT, and the data show that different nitroxyls undergo oxidation at significantly different rates (Figure 8). Their relative rates match the trend expected from their redox potentials: AZADO > ABNO > TEMPO > ACT. Oxidation of ACT is particularly slow, exhibiting a rate 60- and 7-fold slower than those of AZADO and ABNO, respectively, at pH 8.3.

Oxidation of 1-butanol by bleach was then examined by ¹H NMR spectroscopy using the same series of nitroxyls (Figure S8), and the results reveal that these reactions follow the same rate trends observed for oxidation of the nitroxyls by bleach: AZADO > ABNO > TEMPO > ACT. Cyclic chronoamperometry studies illuminate the origin of this trend. Data from the AZADO-, ABNO-, TEMPO-, and ACT-catalyzed alcohol

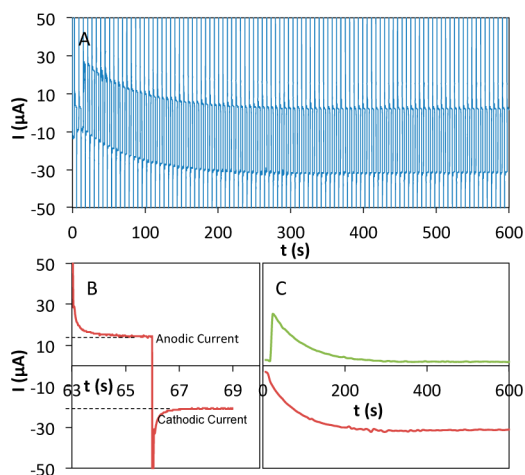


Figure 7. (A) Representative cyclic chronoamperometric data for the oxidation of TEMPO by bleach. (B) Expansion of the oxidation and reduction currents from a single cycle in plot A, obtained from potential steps at 0.71 and 0.25 V vs Ag/AgCl. (C) Plots of the faradaic anodic (positive) and cathodic (negative) currents at each step in plot A (cf. plot B). Pulse width = 3 s, RDE rotation rate = 2000 rpm. Initial concentrations: 5.0 mM TEMPO, 0.2 M NaOCl, 0.12 M NaHCO₃.

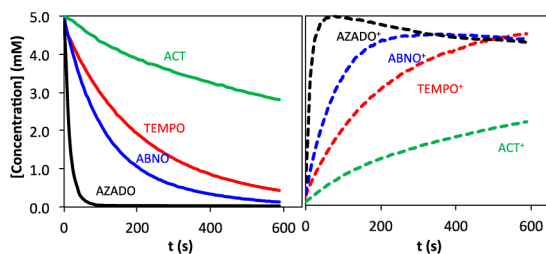


Figure 8. Concentration profiles of nitroxyl and oxoammonium species (solid and dashed lines, respectively) in the presence of bleach, derived from cyclic chronoamperometry. Reaction conditions: 5.0 mM nitroxyl, 120 mM NaOCl, 150 mM NaHCO₃ (pH 8.3).

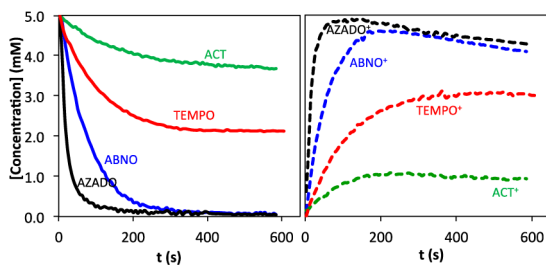


Figure 9. Concentration profiles of nitroxyl and oxoammonium species (solid and dashed lines, respectively) in the oxidation of 1-butanol by bleach, derived from cyclic chronoamperometry. Reaction conditions: 5.0 mM nitroxyl, 100 mM 1-butanol, 120 mM NaOCl, 150 mM NaHCO₃ (pH 8.3).

oxidation reactions, shown in Figure 9, reveal that AZADO and ABNO undergo rapid oxidation to AZADO⁺ and ABNO⁺ and that these oxoammonium species are the predominant form of the catalyst during steady-state turnover. In contrast, TEMPO and ACT convert more slowly to TEMPO⁺ and ACT⁺, and they reach steady-state concentrations of approximately 60% and 20%, respectively. A near-quantitative mass balance of the oxoammonium and nitroxyl species is detected under the different reaction conditions, implying a negligible steady-state

concentration of the hydroxylamine species. (The hydroxylamine formed upon oxidation of the alcohol could undergo rapid oxidation to the nitroxyl by direct reaction with the oxidant or via comproportionation with the oxoammonium species.) Collectively, these observations reveal that the poor catalytic activity of ACT with bleach as the oxidant arises from slow formation of the oxoammonium species (cf. Figure 8). In the electrocatalytic reactions, the electrode potential is adjusted to match the redox potential of the nitroxyl catalyst. Therefore, the catalyst reoxidation rate is normalized for different nitroxyl species and the catalytic rate reflects the intrinsic reactivity of the oxoammonium species with alcohol. The excellent electrocatalytic performance of ACT under basic conditions is attributed to the enhanced electrophilicity of the oxoammonium species ACT⁺, which should favor formation of the alkoxide adduct in the “basic” alcohol oxidation pathway (cf. Scheme 2).

Comparison of Chemical and Electrochemical Nitroxyl-Catalyzed Alcohol Oxidation. The very different catalyst activity trends observed for the bleach- vs electrode-driven alcohol oxidation reactions are depicted in the free-energy correlations in Figure 10. In addition to the four nitroxyls

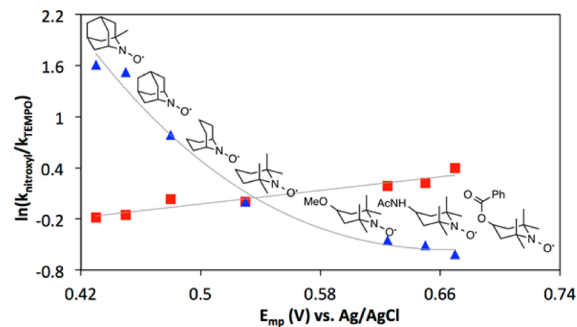


Figure 10. Linear-free-energy correlations for nitroxyl-catalyzed oxidation of 1-butanol with bleach (blue triangles) and under electrochemical conditions (red squares). See Figures S1–S4 and S8 for raw data.

investigated systematically above, three additional nitroxyls 1-Me-AZADO, 4-MeO-TEMPO, and 4-PhCO₂-TEMPO were tested under the same conditions. The bleach-driven reactions (blue triangles) with the seven nitroxyl derivatives show a negative correlation with the nitroxyl E_{mp} values. This trend is attributed to the influence of the catalyst reoxidation step on the overall rate: nitroxyls with lower E_{mp} undergo more-facile oxidation and are therefore more-effective catalysts. The non-linearity of the trend is perhaps expected, considering the turnover-limiting step appears to change across this series of nitroxyls (cf. Figure 9) and/or because ring-strain or steric effects could impact the relative rates for the reactions of nitroxyls with bleach. On the other hand, the electrocatalytic reactions show a small, but positive, correlation with the nitroxyl E_{mp} . The best catalytic rates are obtained with TEMPO derivatives bearing an electron-withdrawing substituent in the 4-position, which have the highest E_{mp} values among the nitroxyls studied. The trend clearly shows that the oxoammonium reduction potential is more significant than steric effects in controlling the reaction rate. The 4-benzoyl derivative exhibits the highest rate among the derivatives tested; however, the ester group is susceptible to hydrolysis under basic conditions. ACT is much less susceptible to hydrolysis and

therefore represents a highly appealing low-cost electrocatalyst for alcohol oxidation.

CONCLUSION

The observations described herein provide extensive insights into the relative activity of TEMPO and bicyclic nitroxyl derivatives, and they have important fundamental and practical implications for this nitroxyl-catalyzed alcohol oxidation reactions. The higher activity of ACT relative to AZADO and ABNO was unexpected, but it shows that increased driving force can compensate for, and even overcome, steric effects in promoting the catalytic activity of nitroxyls. ACT is one of the least expensive nitroxyl derivatives available,⁹ and it exhibits excellent stability and activity over a broad pH range. The results described here bode well for expanded use of ACT in catalytic applications that will leverage the widespread use of ACT⁺ (commonly termed “Bobbitt’s salt”) as a stoichiometric reagent.¹⁸ The exceptional activity of ACT as an electrochemical mediator, particularly at high pH, also provides an important foundation for development of scalable electrocatalytic applications of ACT, for example, via continuous-flow electrolysis.

ASSOCIATED CONTENT

Supporting Information

The Supporting Information is available free of charge on the ACS Publications website at DOI: 10.1021/jacs.5b09672.

Experimental details and additional electrochemical, spectroelectrochemical, and kinetic data, including Figures S1–S8 (PDF)

AUTHOR INFORMATION

Corresponding Author

*stahl@chem.wisc.edu

Notes

The authors declare no competing financial interest.

ACKNOWLEDGMENTS

Financial support for this project was provided by the Great Lakes Bioenergy Research Center (DOE BER Office of Science DE-FC02-07ER64494). Funding for K.C.M. was provided by the NIH (R01 GM100143).

REFERENCES

- (1) For the first application of TEMPO-catalyzed alcohol oxidation and a comprehensive survey, see: (a) Cella, J. A.; Kelley, J. A.; Kenehan, E. F. *J. Org. Chem.* **1975**, *40*, 1860. (b) Bobbitt, J. M.; Brückner, C.; Merbouh, N. *Org. React.* **2009**, *74*, 103.
- (2) For a review, see: Ciriminna, R.; Pagliaro, M. *Org. Process Res. Dev.* **2010**, *14*, 245.
- (3) For reviews, see: (a) de Nooy, A. E. J.; Besemer, A. C.; van Bekkum, H. *Synthesis* **1996**, 1996, 1153. (b) Sheldon, R. A.; Arends, I. W. C. E. *Adv. Synth. Catal.* **2004**, *346*, 1051. (c) Tebben, L.; Studer, A. *Angew. Chem., Int. Ed.* **2011**, *50*, 5034. (d) Wertz, S.; Studer, A. *Green Chem.* **2013**, *15*, 3116. (e) Ryland, B. L.; Stahl, S. S. *Angew. Chem., Int. Ed.* **2014**, *53*, 8824. (f) Cao, Q.; Dorman, L. M.; Rogan, L.; Hughes, N. L.; Muldoon, M. *Chem. Commun.* **2014**, *50*, 4524. (g) Seki, Y.; Oisaki, K.; Kanai, M. *Tetrahedron Lett.* **2014**, *55*, 3738. (h) Miles, K. C.; Stahl, S. S. *Aldrichimica Acta* **2015**, *48*, 8.
- (4) For leading references, see: (a) Semmelhack, M. F.; Chou, C. S.; Cortes, D. A. *J. Am. Chem. Soc.* **1983**, *105*, 4492. (b) Osa, T.; Kashiwagi, Y.; Mukai, K.; Ohsawa, A.; Bobbitt, J. M. *Chem. Lett.* **1990**, *19*, 75. (c) Kashiwagi, Y.; Kurashima, F.; Kikuchi, C.; Anzai, J.; Osa, T.;

Bobbitt, J. M. *Tetrahedron Lett.* **1999**, *40*, 6469. (d) Liaigre, D.; Breton, T.; Belgsir, E. M. *Electrochem. Commun.* **2005**, *7*, 312. (e) Hill-Cousins, J. T.; Kuleshova, J.; Green, R. A.; Birkin, P. R.; Pletcher, D.; Underwood, T. J.; Leach, S. G.; Brown, R. C. D. *ChemSusChem* **2012**, *5*, 326. (f) Green, R. A.; Hill-Cousins, J. T.; Brown, R. C. D.; Pletcher, D.; Leach, S. G. *Electrochim. Acta* **2013**, *113*, 550. (g) Hickey, D. P.; McCammant, M. S.; Giroud, F.; Sigman, M. S.; Minter, S. D. *J. Am. Chem. Soc.* **2014**, *136*, 15917. (h) Rafiee, M.; Karimi, B.; Alizadeh, S. *ChemElectroChem* **2014**, *1*, 455. (i) Cha, H. G.; Choi, K.-S. *Nat. Chem.* **2015**, *7*, 328. (j) Hickey, D. P.; Milton, R. D.; Chen, D.; Sigman, M. S.; Minter, S. D. *ACS Catal.* **2015**, *5*, 5519.

(5) For a review, see: Ciriminna, R.; Palmisano, G.; Pagliaro, M. *ChemCatChem* **2015**, *7*, 552.

(6) Numerous examples are included in the reviews in ref 3. See also: (a) Siedlecka, R.; Skarzewski, J.; Młochowski, J. *Tetrahedron Lett.* **1990**, *31*, 2177. (b) de Nooy, A. E. J.; Besemer, A. C.; van Bekkum, H. *Tetrahedron* **1995**, *51*, 8023. (c) Hoover, J. M.; Stahl, S. S. *J. Am. Chem. Soc.* **2011**, *133*, 16901.

(7) Bailey, W. F.; Bobbitt, J. M.; Wiberg, K. B. *J. Org. Chem.* **2007**, *72*, 4504.

(8) For leading references, see refs 3e, 3h, and the following: (a) Graetz, B.; Rychnovsky, S.; Leu, W.-H.; Farmer, P.; Lin, R. *Tetrahedron: Asymmetry* **2005**, *16*, 3584. (b) Shibuya, M.; Tomizawa, M.; Suzuki, I.; Iwabuchi, Y. *J. Am. Chem. Soc.* **2006**, *128*, 8412. (c) Demizu, Y.; Shiigi, H.; Oda, T.; Matsumura, Y.; Onomura, O. *Tetrahedron Lett.* **2008**, *49*, 48. (d) Kuang, Y.; Rokubuchi, H.; Nabae, Y.; Hayakawa, T.; Kakimoto, M.-a. *Adv. Synth. Catal.* **2010**, *352*, 2635. (e) Shibuya, M.; Osada, Y.; Sasano, Y.; Tomizawa, M.; Iwabuchi, Y. *J. Am. Chem. Soc.* **2011**, *133*, 6497. (f) Steves, J. E.; Stahl, S. S. *J. Am. Chem. Soc.* **2013**, *135*, 15742. (g) Lauber, M. B.; Stahl, S. S. *ACS Catal.* **2013**, *3*, 2612. (h) Sasano, Y.; Nagasawa, S.; Yamazaki, M.; Shibuya, M.; Park, J.; Iwabuchi, Y. *Angew. Chem., Int. Ed.* **2014**, *53*, 3236.

(9) Prompted by a reviewer’s request, we provide the cost for 1 mmol of the commercially available nitroxyls considered in this study (prices reflect the lowest available cost from Sigma-Aldrich at <http://www.sigmaaldrich.com/>, accessed Sept 11, 2015): TEMPO (\$0.83), ACT (\$0.96), 4-MeO-TEMPO (\$5.69), 4-oxo-TEMPO (\$7.14), 4-PhCO₂-TEMPO (\$16.81), ABNO (\$32.76), AZADO (\$155.64), 1-Me-AZADO (\$328.68). The cost of individual nitroxyls will, of course, depend upon the scale of production.

(10) See refs 3d, 3g, 8f, 8g, and the following: Xie, X.; Stahl, S. S. *J. Am. Chem. Soc.* **2015**, *137*, 3767.

(11) Gerken, J. B.; Stahl, S. S. *ACS Cent. Sci.* **2015**, *1*, 234.

(12) For redox potentials of diverse nitroxyls, see ref 8g and the following: (a) Shchukin, G. I.; Ryabinin, V. A.; Grigorev, I. A.; Volodarskii, L. B. *J. Gen. Chem. U.S.S.R.* **1985**, *56*, 753. (b) Bobbitt, J. M.; Flores, M. C. L. *Heterocycles* **1988**, *27*, 509. (c) Shibuya, M.; Pichierri, F.; Tomizawa, M.; Nagasawa, S.; Suzuki, I.; Iwabuchi, Y. *Tetrahedron Lett.* **2012**, *53*, 2070.

(13) Golubev, V. A.; Sen, V. D. *Russ. J. Org. Chem.* **2011**, *47*, 869.

(14) The rate of the catalytic reaction can be derived from the following equation:

$$I_{\text{cat}} = nFAC_{\text{N}}(D_{\text{A}}k_{\text{obs}}C_{\text{A}})^{1/2}$$

I_{cat} represents the catalytic current, C_{N} and C_{A} are the bulk concentrations of nitroxide and alcohol, and n , F , and A denote the number of electrons, Faraday constant, and electrode surface area, respectively. The amount of $5.0 \times 10^{-6} \text{ cm}^2 \text{ s}^{-1}$ has been considered as the diffusion coefficient (D_{A}) of all alcohols. See ref 4h and the following: Costentin, C.; Drouet, S.; Robert, M.; Savéant, J.-M. *J. Am. Chem. Soc.* **2012**, *134*, 11235.

(15) The results in Table 2 are included to demonstrate that ACT can serve as an effective electrocatalytic mediator under bulk electrolysis conditions. Ongoing studies are focused on optimizing these conditions for synthetic applications, including consideration of the preferred electrochemical apparatus and the substrate scope and functional group compatibility.

(16) (a) Golubev, V. A.; Sen, V. D.; Rozantsev, É. G. *Bull. Acad. Sci. USSR, Div. Chem. Sci.* **1979**, *28*, 1927. (b) Fish, J. R.; Swarts, S. G.; Sevilla, M. D.; Malinski, T. J. *Phys. Chem.* **1988**, *92*, 3745.

(17) For relevant examples, see ref [12c](#) and the following: Hamada, S.; Furuta, T.; Wada, Y.; Kawabata, T. *Angew. Chem., Int. Ed.* **2013**, *52*, 8093.

(18) Mercadante, M. A.; Kelly, C. B.; Bobbitt, J. M.; Tilley, L. J.; Leadbeater, N. E. *Nat. Protoc.* **2013**, *8*, 666.